**Aalborg Universitet**



# Sharing sequence components of reactive power in a three-phase four-wire islanded microgrid

Ashish Shrestha

[Link to publication from Aalborg University](Link to publication from Aalborg University)

# Sharing sequence components of reactive power in a three-phase four-wire islanded microgrid

**Binod Sharma[a,*], Ashish Shrestha[b], Yacine Terriche[c], Abderezak Lashab[c], Josep M. Guerrero[c]**

[a]Modikhola Hydropower Plant, Nepal Electricity Authority, Dimuwa, Parbat 33400, Gandaki, Nepal

[b]Department of Electrical Engineering, Information Technology and Cybernetics, University of South-Eastern Norway, Porsgrunn, N-3918, Norway

[c]AAU Energy, Aalborg University, Aalborg, 9220, Denmark

*Corresponding author: binodsha84@gmail.com (Binod Sharma)

*Abstract*

Under any load disturbances, the microgrid must maintain its voltage and frequency within the standard norms. In an isolated microgrid, under-loading and overloading conditions may emerge if the sequence components of powers are not appropriately shared by the power electronics interfaced distributed generation systems (DGSs). Hence, this paper tends to offer a droop-based control strategy for a three-level neutral point clamped (NPC) inverters-based islanded microgrid that enables supply and maintains power-sharing effectively. The proposed method constitutes enhanced voltage and current controllers, sequence components-based virtual impedance (VI) loop, and frequency restoration loop. With the proposed droop-based control, an equal and proportional power-sharing is achieved. Furthermore, the presented VI loop allows the connected DGs with uneven line impedances to share the positive and negative sequence components of the reactive power under unbalanced loads. Besides, the upgraded voltage controllers in the stationary reference frame ensure that the DG's terminal voltages remain balanced, even when the loads at point of common coupling (PCC) demand uneven currents, while the frequency restoration loop maintains the system frequency very close to the nominal value (i.e., 50Hz). Various scenarios such as equal and proportional power sharing and multiple numbers of DGs are considered in the study to validate the efficacy of the proposed control scheme. The simulation results are carried out in MATLAB/Simulink environment to demonstrate the efficiency of the suggested control scheme.

*Keywords:* Droop control; Virtual impedance; Sequence power-sharing; Proportional power-sharing; Frequency restoration

## 1. Introduction

The loads in an islanded microgrid are often single-phase and unbalanced [1]. With imbalanced loads, there are both positive and negative sequence powers [2]. A condition of under-loading and overloading may occur if these sequence powers are not correctly shared among the participating distributed generations (DGs). Islanded microgrids maintain their voltage and frequency stable on their own in case a disturbance occurs [3, 4]. When loads at the point of common coupling (PCC) draw unbalanced currents, DGs must keep their terminal voltages balanced, uniform, and equal to minimize wasteful current circulation between the DGs [5-7]. The inclusion of a low pass filter in an inverter-based DG

results in a higher internal impedance which causes a noticeable unbalance in the terminal voltages of inverter-based DGs [8].

Active power/frequency (P/F) and reactive power/voltage (Q/V) droop-based control approaches comprising inner current and voltage controllers are the most prevalent control schemes for an islanded microgrid. It does, however, have several drawbacks, including line impedance dependence, intrinsic voltage and frequency droop, poor transient and unbalanced power-sharing, and a trade-off between voltage regulation and power-sharing. Virtual impedance is a concept presented to overcome problems caused by impedance mismatch [9]. An adaptive transient droop function is combined with conventional droop control to improve transient response and power-sharing stability in [10]. A fundamental positive sequence (FPS) based control strategy comprising proportional-integral (PI) plus multi-resonant voltage controller integrated within the power droop loops for improving unbalanced and harmonic power-sharing is proposed in [11]. Moreover, the droop-based control scheme requires a secondary control loop to restore the inherent deviations created on voltage and frequency [12]. Several studies attempted in different aspects to make the conventional virtual impedance concept more effective by compensating the impedance mismatch effect. An adaptive virtual impedance that doesn't require the actual value of line impedance to be known is proposed in [13]. A selective virtual impedance loop based on both positive and negative sequence components is implemented to improve the current-sharing under non-linear loads [14]. However, the latter ignores zero sequence current in virtual impedance implementation and uses only the virtual resistance for negative sequence components. Hence, it is required to balance the DGs' neutral currents, in the case of three-phase-four-wire systems considering the zero sequence components, which are quite a popular microgrid's topology. Active power filter concepts and many voltage compensation methods involve an injection of negative sequence voltage to improve the voltage profile during unbalance [15-17]. However, these methods don't enhance unbalanced power sharing effectively. Therefore, a method based on the proper output impedance control of DG using a $Q^{-}$-Z controller is proposed in [18]. However, it ignores the fact that lines usually have different impedances, which affects both positive and negative sequence reactive power sharing.

This paper aims to propose an enhanced droop-based control scheme to improve the reactive power-sharing of three-level neutral point clamped (NPC) inverters-based three-phase-four-wire islanded microgrids under unbalanced loads. The three-phase four-wire configuration is a universally adopted system for low voltage distribution due to its neutral in the system, which offers several advantages in terms of power quality, protection, and flexibility. The three-level NPC inverters are selected for enhancing the three-phase-four-wire microgrid over two-level inverters as they do not require an extra limb for the neutral, have reduced stresses on the switches on high power applications, and have low harmonic content in the outputs [19]. Besides, a virtual impedance loop based on the sequence components has been investigated that enables the sharing of positive and negative sequence reactive power among the DGs by compensating the impedance mismatch effect more effectively. Extraction of sequence components is realized with the help of a second-order general integrator (SOGI) [20]. The proposed virtual impedance also helps to balance the DGs' neutral currents under unbalanced power-sharing. The voltage reference obtained from the droop controller is tracked with the help of proportional-resonant (PR) controllers in αβ0-axes. The use of PR controllers in αβ0-axes in the voltage and current controllers helps to diminish the effects of the neutral voltage shifting and zero sequence component to guarantee a balanced and stable voltage with an optimum power-sharing under unbalanced loads.

Furthermore, a frequency restoration loop is incorporated in the proposed control scheme to regain the nominal frequency after every load change. Enhancement of reactive power-sharing with the proposed VI loop has no appreciable impact on active power-sharing. Thus, the proposed droop-based control technique accomplishes the division of total connected load among the DGs. The control scheme is validated through simulation of different case scenarios. Though described in detail in further chapters, the main contributions of this paper are related to:

a. This paper developed a droop-based control technique for a three-level NPC inverters-based three-phase four-wire microgrid. This control technique is proposed for an islanded microgrid with multiple DGs that frequently experience unbalanced loads. Using simulation analysis, the proposed control technique is found to be effective in maintaining power-sharing as well as power quality. Improved voltage and current controllers, a sequence components-based virtual impedance (VI) loop, and a frequency restoration loop are all part of the proposed strategy.

b. A sequence components-based virtual impedance loop has been proposed to make sure there were no voltage drop mismatches in the lines and to make sure the positive and negative sequence components of reactive power were shared appropriately. It also helps to balance the currents in the DGs' neutrals flowing due to the unbalanced loads.

c. A viable concept for an isolated microgrid has been developed, with the distribution system operating in a three-phase four-wire mode. Various scenarios such as equal and proportional power sharing and multiple numbers of DGs have been studied in order to assess the proposed method's performance and robustness.

d. On both the voltage and current control loops, multiple root-loci sweeps and time-domain responses have been performed to ensure the stability of the proposed controller while achieving good performance during both steady-state and transients. This research ensures the proposed method's stability in various modes and scenarios.

The whole body of this paper is organized as follows: Section 1 presents the general overview of the control strategy and the research gaps. The adopted method along with a detailed block diagram and mathematical modeling are described in Section 2. The simulation results are discussed in Section 3. The conclusion of this study is presented in Section 4.

## 2. Method

### 2.1 Test microgrid layout

The layout of the test microgrid system is shown in Figure 1. Two parallel identical DGs are connected to PCC through the lines. A three-level NPC inverter with a fixed DC voltage source in its input and a low pass LC filter in its output is considered as a DG. As shown in Figure 1, the DC side neutral of the inverter is taken to AC side PCC and the three-phase-four-wire microgrid is formed. Reduced stress on switches, better power rating capability, low harmonic content in the outputs, ride-through capability, increased dynamic performance, higher efficiency, lower cost, and no extra limb required for the neutral are all advantages of three-level NPC inverters made out of insulated-gate bipolar transistor (IGBT) and diodes [19, 21]. DGs are placed at unequal distances from the PCC. Balanced and single-phase or unbalanced loads are supplied from the PCC. Low pass LC filters are used to minimize higher-order harmonics in the inverter output [22, 23]. The LC filters used in the paper are passive damping types, and

the value of the inductor filter is selected in such a way so that the voltage drop across it remains within 3% of the inverter output voltage. The value of capacitor filter is calculated from the resonant frequency considering the following conditions: (a) $10 \times f_0 < f_r < (1/10) \times f_{sw}$, and (b) $I_{lmax} \times (2\pi f L) < 0.03 \times V_{inv}$. Where, $I_{lmax}$ is the maximum root mean square (RMS) value of the load current, $f$ is the frequency of the output voltage, $V_{inv}$, $f_r$ is resonant frequency, $f_0$ is fundamental frequency, and $f_{sw}$ is switching frequency.
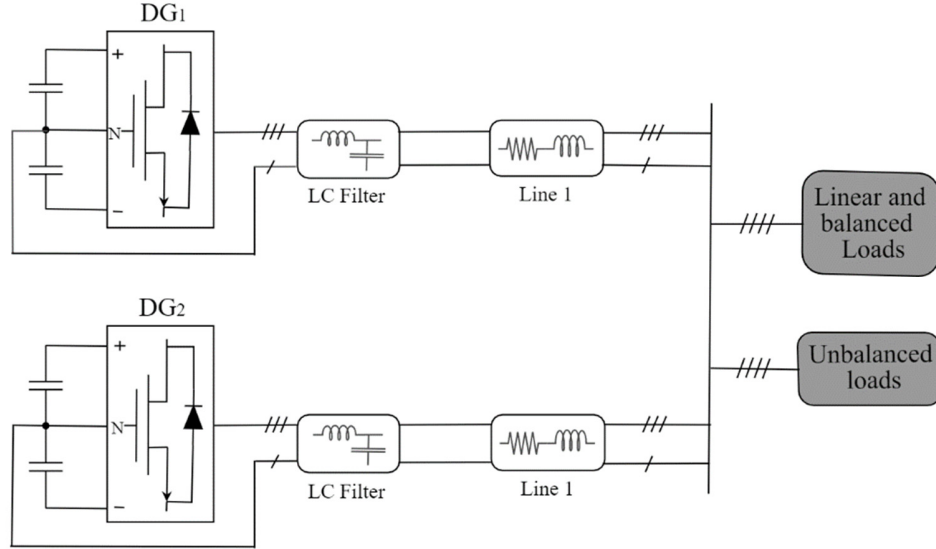


Figure 1: Layout of test microgrid

## 2.2 Sequence power calculation

Three-phase instantaneous active power has been calculated by just multiplying phase currents with corresponding phase voltages and summing all the phase powers. Accurate reactive power for an unbalanced system has been calculated by introducing a 90-degree phase delay in voltage and multiplying it with the current. The phase delay in voltage is introduced with the help of second-order generalized integrator (SOGI) [24, 25]. The positive and negative sequence powers for unbalanced load conditions are calculated in the $\alpha\beta0$-reference frame from the respective sequence components of current and voltage [26]. Positive and negative sequence components of current and voltage are extracted from SOGI-based bandpass filter (BPF) [20], and sequence powers are calculated as shown in Figure 2.

$$P\pm = V\alpha \times I\alpha + V\beta \times I\beta \tag{1}$$

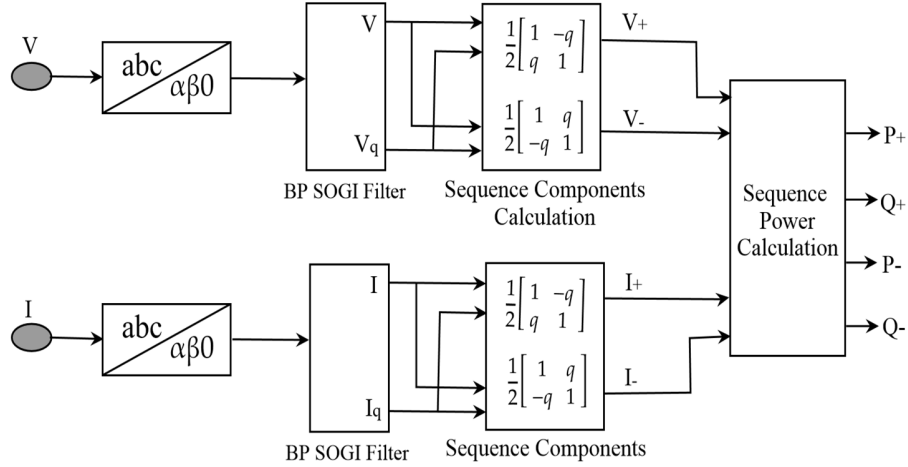$$Q\pm = V\beta \times I\alpha - V\alpha \times I\beta \tag{2}$$

Figure 2: SOGI-based bandpass filter for sequence power calculation

## 2.3 Overall controller section

The block diagram of the overall controller section proposed in this paper is shown in Figure 3. The Controllers are identical for both DGs except a virtual impedance loop is incorporated only in the voltage controller of the DG having smaller line impedance. Three-phase instantaneous active and reactive powers are calculated with the measurement of DG terminal voltages and currents. These calculated powers are used in the droop controller to obtain the magnitude and phase of the voltage reference. A three-phase sinusoidal voltage reference signal is generated with phase and magnitude obtained from the droop controller. The voltage reference signal is tracked in the voltage controller with proportional resonant (PR) controller in $\alpha\beta0$- axes. It regulates the voltage and eliminates the unbalance. Thus, it enables the voltage source inverter (VSIs) to operate in the islanded mode with unbalanced loads. The PR controllers offer minimum steady-state error and selected harmonic rejection capability [27]. The voltage controller acts as a restoration loop for the droop voltage during the operation of the droop controller. A frequency restoration loop based on the deviation of the phase angle is proposed to restore the frequency to its nominal value. The concept of virtual impedance for impedance matching is also introduced in this voltage controller that increases the line impedance of the DGs having a lower value of line impedance. The virtual voltage drop that matches the line voltage drop, is calculated by multiplying positive, negative, and zero sequence line currents with the respective impedances. It enables the sharing of sequence reactive powers more accurately. The output of the voltage controller is used as the reference for the inner current controller. The output of the inner current controller is transformed back to the abc-reference frame and fed to a three-level pulse width modulation (PWM) generator. The pulse generated by the PWM generator is used to control the three-level NPC inverter. The controller segments used are described in detail in the following sub-sections:
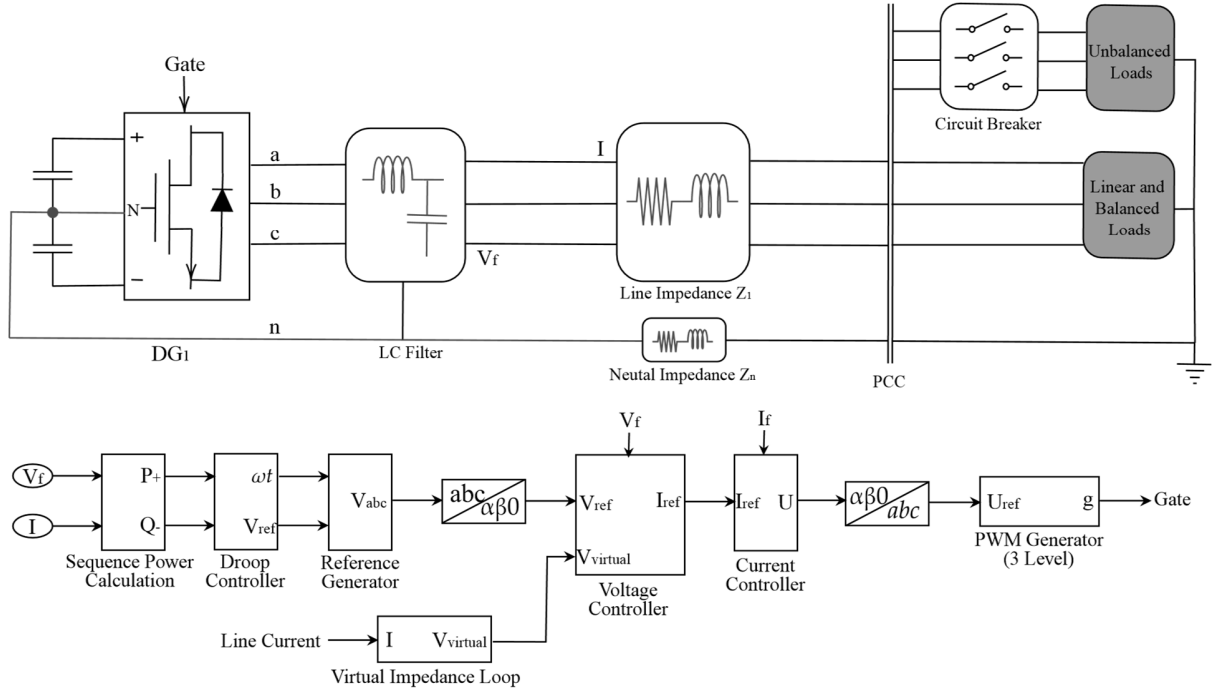
Figure 3: Block diagram of the overall controller section

### A. Droop-based control system

The droop control technique is based on the operation of an alternator and is widely used as an independent and distributed control for an inverter-based microgrid. Derivation of droop equations is described in detail in [24]. The conventional droop equations for $P/\phi$ & $Q/V$ droop derived from the static power flow equations are given below:

$$\phi = \phi^* - mP \tag{3}$$

$$E = E^* - nQ \tag{4}$$

Equation (3) is modified to act as a proportional-derivative controller for the frequency and improve the dynamic behavior of the power-sharing [24].

$$\phi = \phi^* - (m_p P + m_i \int P dt) \tag{5}$$

The issues of conventional droop control methods such as inherent voltage and frequency droop, the effect of line impedance mismatch and inaccurate unbalance power-sharing are addressed suitably in this paper.

### B. Frequency restoration

There is always some inherent droop in frequency in a droop-controlled microgrid, whenever the active load of the system increases. Frequency deviation has a standard permissible limit of 2.5%, but practically frequency is kept almost constant very close to the nominal value of 50 Hz. It is advantageous to keep frequency very close to the nominal value rather than at the marginal value to reduce the risk of system stability due to unexpected fluctuations. Thus, in this paper, a simple frequency restoration block based

on the deviation of the phase angle ($\delta$) is introduced, which restores the frequency to the nominal value after each load disturbance. Basically, it is a secondary controller that acts after the droop controller. For the implementation, a very simple concept of frequency restoration has been used which measures deviation of the frequency droop output from the nominal value. It acts on the output of the $P/\phi$ droop controller and produces a modified phase reference to the reference generator. The block diagram of frequency restoration is shown in Figure 4. The deviation on frequency is used to bring the output frequency back to the nominal value. The system frequency can be made approximately uniform despite the load change by choosing a very small $P/F$ droop coefficient, but it makes the system insensitive and active power sharing accuracy is affected. Thus, it is advantageous to have relatively larger droop coefficients and a frequency restoration loop.
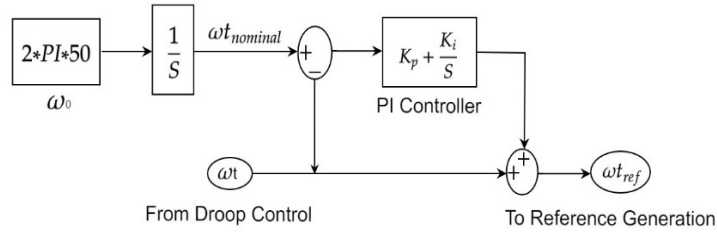


Figure 4: Block diagram of frequency restoration

## C. Sequence components-based virtual impedance

When the line impedances of participating DGs are different, unequal voltage drops occur across the lines which leads to cause circulation of current between the DGs and thus results in improper sharing of powers (mainly reactive power). The Concept of virtual impedance is introduced to sort out the problems created by unequal line impedances. Virtual voltage drop that balances the voltage drop in the lines is incorporated in the controller using virtual values of the line impedance. Generally, the line impedance of the DG having lower line impedance is virtually increased. In this study, the value of virtual impedance required for $DG_1$, $Z_{1V}$ is calculated using (6).

$$Z_{1\,V} \;\; = \;(S_2/S_1) \times (Z_2 - Z_1) \tag{6}$$

Where $S_2/S_1$ is the ratio of load sharing, and $Z_1$ and $Z_2$ are the impedances of lines connecting the DGs and PCC. The conventional virtual impedance is not suitable for sharing sequence powers as it doesn't differentiate the sequence components. Thus, a virtual impedance loop based on the sequence components for proper sharing of both positive and negative sequence components of power is proposed in this paper. SOGI-BP filters are used for the extraction of sequence components. The block diagram of the proposed virtual impedance implemented in the $\alpha\beta0$-reference frame is shown in Figure 5. An impedance is placed in the 0-axis of $\alpha\beta0$-reference frame in the virtual impedance loop to balance the currents in the DGs neutrals.

## D. Inner current and voltage controllers

The block diagrams of the inner current and voltage controllers implemented in the $\alpha\beta0$-reference frame are shown in Figures 6 and 7. The reference signal given by the droop controller is used to regulate the DGs voltages and currents with PR controllers. The voltage controller acts as a restoration loop for

voltages and maintains a balance for harmonic free voltage profile. The inner current and voltage controllers proposed in [26], are modified to make them suitable for a three-phase four-wire system [28]. The PR controllers, being suitable for tracking the references with zero steady-state error in $\alpha\beta0$-reference frame are used in this paper. Virtual voltage drop is subtracted from the reference obtained from droop control in the controller of the DGs having lower line impedance. One additional PR controller in the 0-axis of $\alpha\beta0$-reference frame is used to regulate the shifting of neutral voltage in the voltage controller. The output of the voltage controller is tracked by an inner current controller. The effect of the unbalanced current flowing in the neutral is compensated with a PR controller in 0-axis of $\alpha\beta0$- reference in the inner current controller.
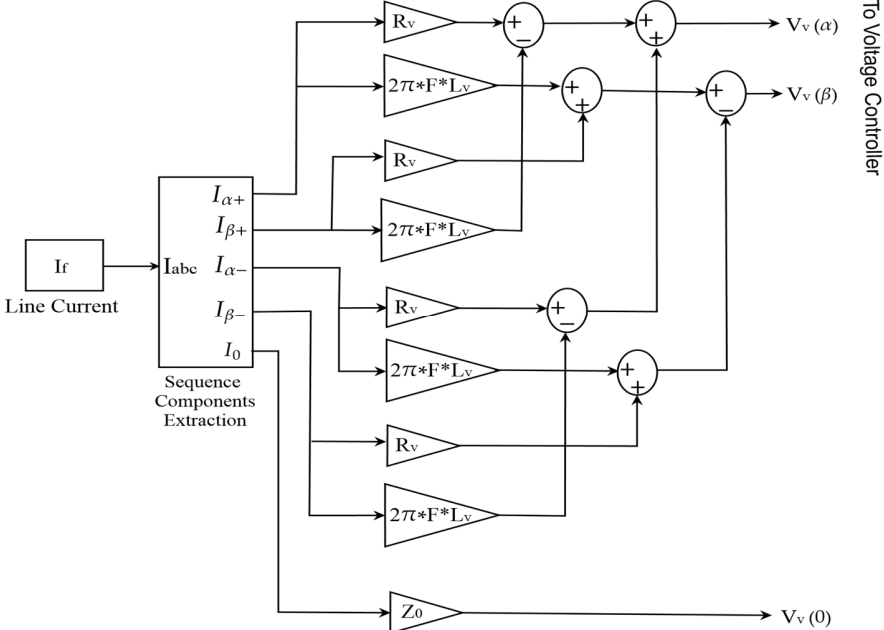


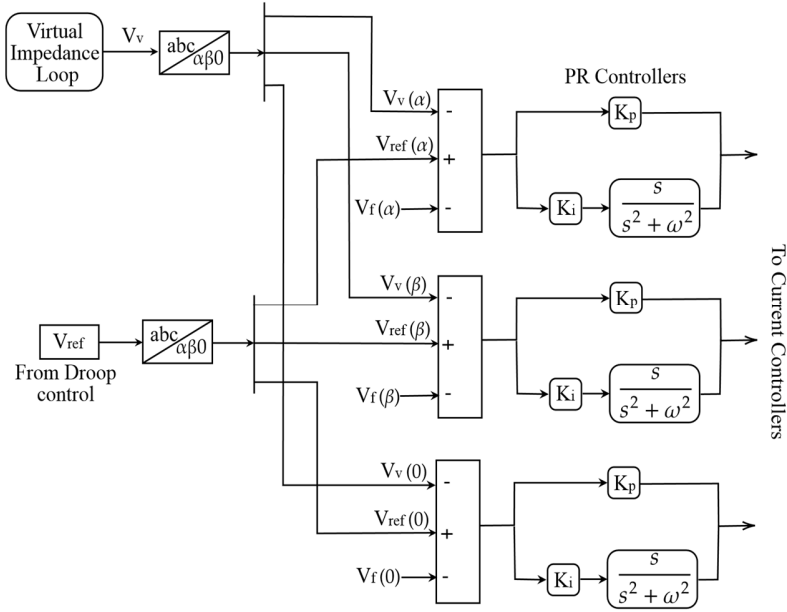Figure 5: Sequence components based virtual impedance

Figure 6: Block diagram of the inner voltage controller
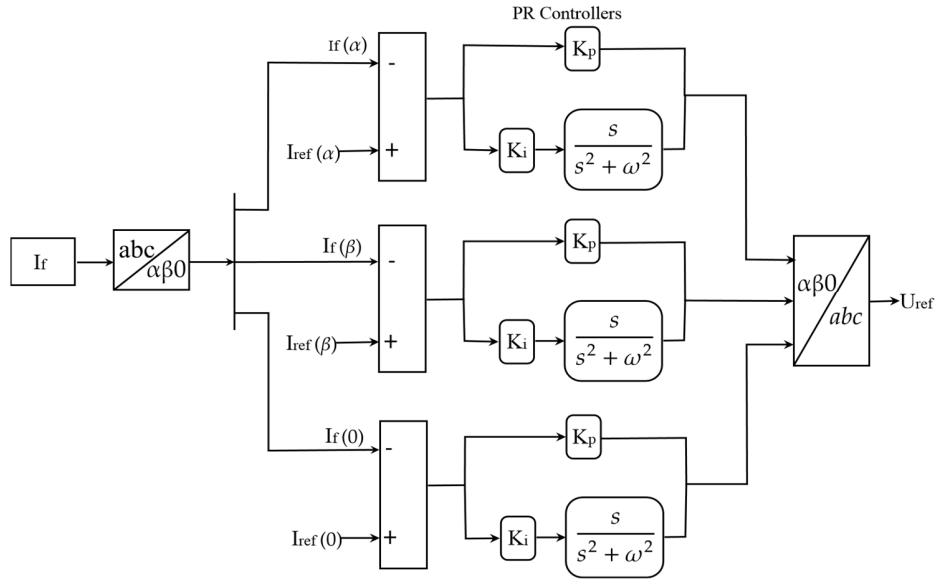


Figure 7: Block diagram of the inner current controller

## 3. Result and Discussion

The presented model of test microgrid and controllers have been simulated in MATLAB/Simulink software. The parameters used in this study are listed in Table 1. Two different scenarios of equal and proportional power-sharing are considered to show the characteristics of the proposed model in different load conditions. The DG terminal voltages, currents, system frequency, positive and negative sequence active and reactive powers for both of the scenarios have been determined and discussed in detail.

Table 1: Parameters of simulation setup

| Description of Parameters | Value |
|---|---|
| $V_{dc}$ | 800 V |
| PWM switching frequency | 18,000 Hz |
| Filter L and C | 1.46 mH and 30.8 $\mu$F |
| Line Impedance $L1$ and $L2$ | $0.2 + j0.6$ and $0.4 + j1.2$ |
| Neutral line impedance, $L_{n1}$ and $L_{n2}$ | $0.2 + j0.6$ and $0.4 + j1.2$ |
| Droop coefficients m, $m_p$ and n | 0.001, 0.001 and 0.0012 |
| Virtual Impedance $Rv$, $Xv$, and $Z_{0v}$ | 0.2, 0.6 and 1.44 |
| Voltage controller gains $K_p$, $Ki$ | 0.45 and 35 |
| Current controller gains $K_p$, $K_i$ | 1 and 800 |
| Frequency Restoration Gain coefficients $K_p$ and $K_i$ | 0.998 and 0.02 |

## 3.1. Performance analysis for equal power-sharing

In this scenario, two DGs of equal capacity are used with identical droop coefficients, which are selected for both controllers to achieve equal power-sharing. In this paper, the values are chosen by considering the standard voltage variation limit of 10%, frequency variation limit of 2.5%, and the expected system load change. The overall test system is simulated for three seconds: initially, only balanced loads are supplied from the PCC, and then unbalanced loads are connected to the system after one second. The information on ratings and switching of the loads are summarized in Table 2.

Table 2: Simulation parameters used in scenario 1

| Description of Parameters | Value | Remarks |
|---|---|---|
| PCC balanced load, P(w)+jQ(var) | 6000+j2400 | Always connected |
| PCC unbalanced load, P(w)+jQ(var) | Phase A: 2000+j800, Phase B: 4000+j1600, Phase C: 6000+j2400 | Connected to PCC from one second to two seconds of the simulation. |

The simulation results are obtained for different controllers and compared with the proposed one. As DGs are provided with identical droop coefficients, an equal sharing of positive and negative sequence powers is expected. With the conventional virtual impedance, acceptable positive sequence reactive power-sharing is achieved which is shown in Figure 8(a). As shown in Figure 8(a), the positive sequence reactive power shared by both DGs are inline. However, equal sharing of the negative sequence reactive

power is not achieved. A significant difference in the negative sequence reactive power-sharing for two DGs can be seen in Figure 8(c). The $DG_1$ having lower line impedance couldn't even share as much negative sequence reactive power as $DG_2$ does. It indicates that the use of a conventional virtual impedance loop overcompensates the effect of impedance difference in the negative sequence power-sharing. Whereas with the proposed virtual impedance loop, the virtual voltage drop required to balance the impedance mismatch is calculated in both sequence components separately by taking the respective sequence components of current. The proposed virtual impedance loop assists in achieving improved positive and negative sequence power-sharing. Thus, both DGs have shared equal reactive powers, which can be seen in Figures 8(b & d). Here in Figure 8(b & d), both the positive and negative sequence reactive power-sharing are in the same line; both DGs share the same loadings. In addition, the impedance difference doesn't cause any appreciable impact on active power-sharing. The active power has been shared equally between the participating DGs with great accuracy when the proposed control technique is implemented. It can be seen in Figure 9, the active power-sharing by both DGs are in the same line.
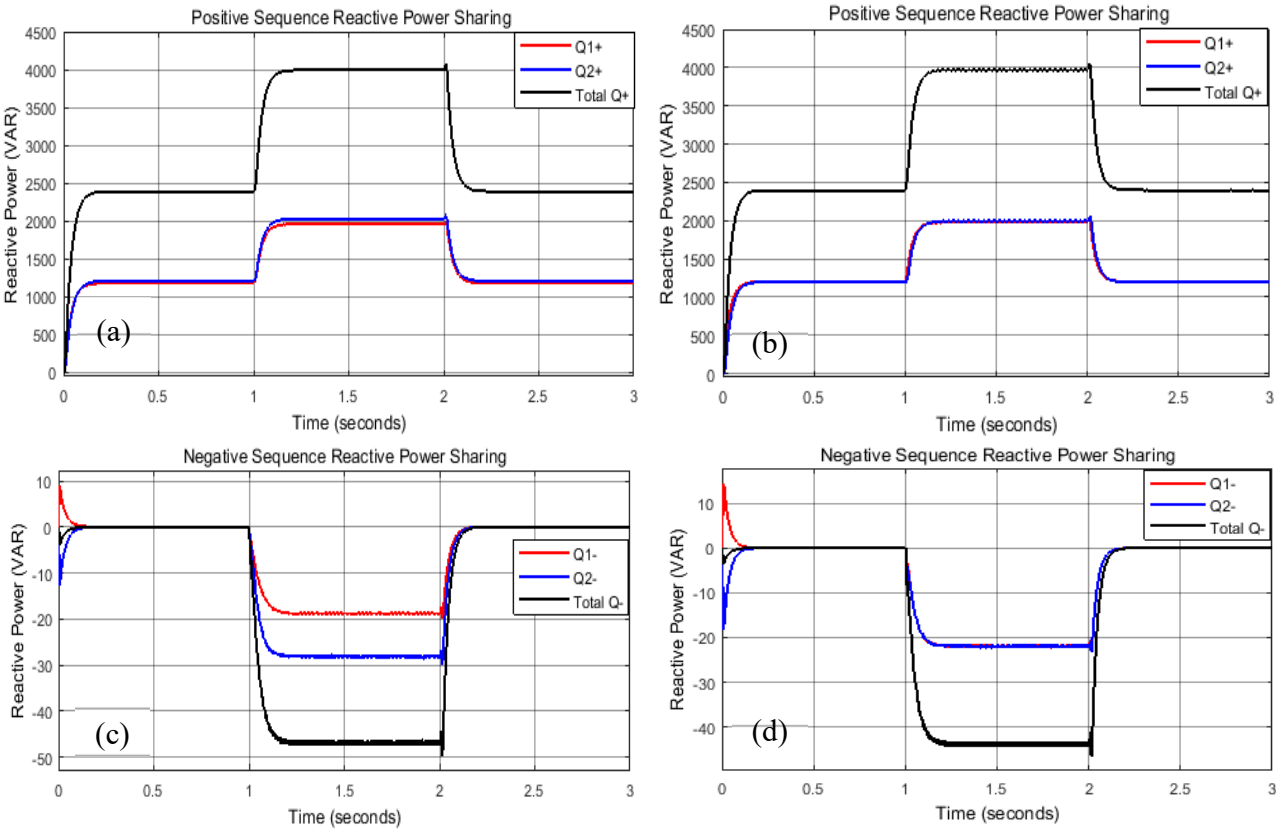


Figure 8: Reactive power-sharing: (a) Positive sequence with conventional VI loop, (b) Positive sequence proposed VI loop, (c) Negative sequence with conventional VI loop, and (d) Negative sequence with proposed VI loop
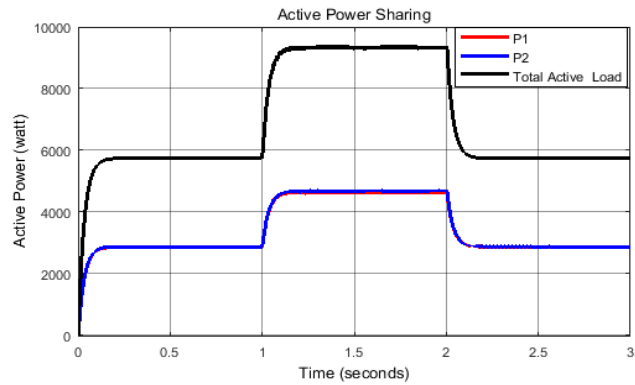
Figure 9: Active power-sharing the proposed control strategy

The DGs in a microgrid need to maintain their terminal voltages in a balanced condition even if the unbalanced loads are added at the PCC. This is very essential as the DGs may have sensitive loads at their terminals demanding a balanced voltage for their operation. The natures of terminal voltages and currents through the DGs with the proposed scheme are shown in Figure 10. As shown in Figure 10, balanced and sinusoidal voltages are maintained in each DG terminal throughout the considered time, even the unbalanced loads are supplied from the PCC. As the DGs have shared an equal amount of powers, the DG currents are identical. As shown in Figure 10(b), DG's currents are unbalanced for the duration when unbalanced loads are supplied (i.e., from one second to two seconds).



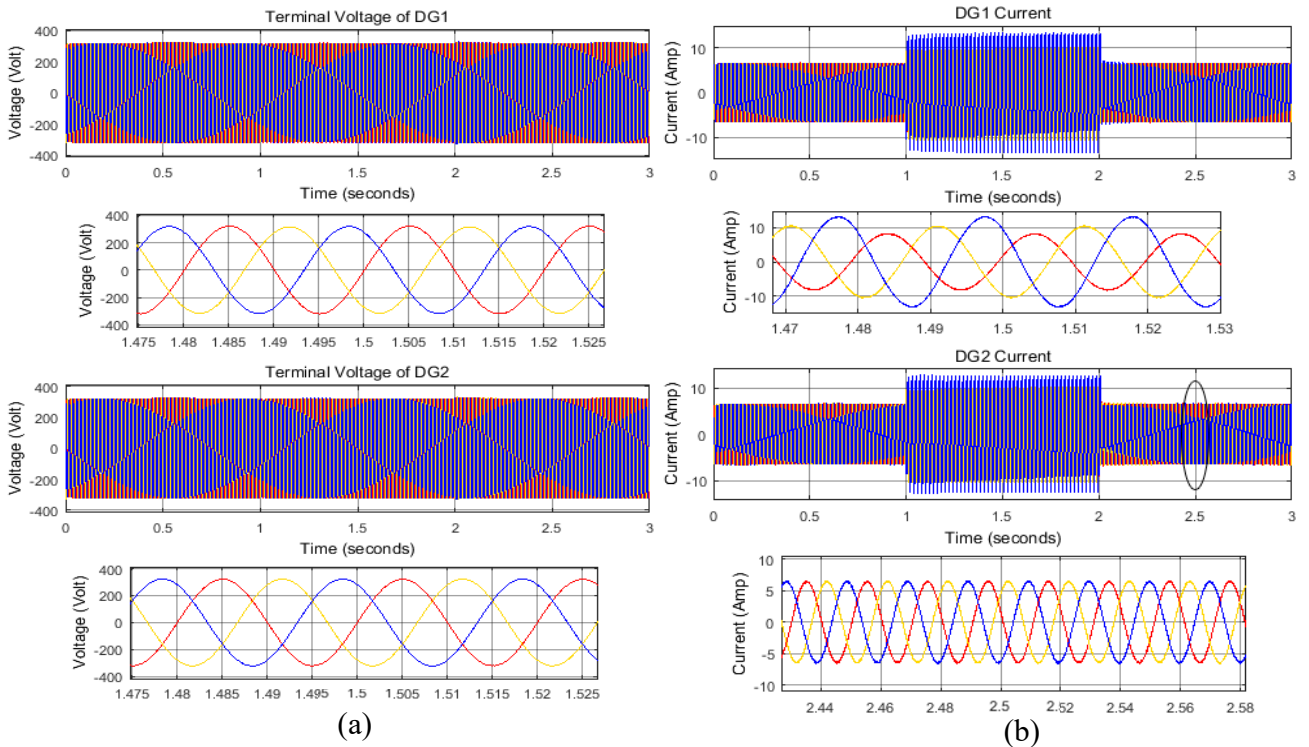(a)                                           (b)

Figure 10: DG's terminal voltages and currents with the proposed control strategy
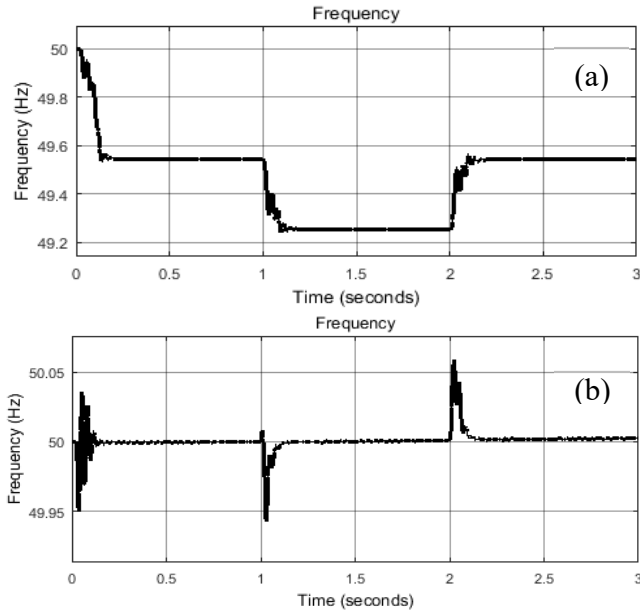
Figure 11: System frequency: (a) Without frequency restoration, (b) With frequency restoration

Similarly, in the droop-controlled microgrid, the system frequency decreases when the active power load is added to the system and increases whenever the active power load is removed from the system. However, it is very crucial to preserve the system frequency very close to the nominal value from the perspective of system stability. In this study, the system frequency is immediately brought back at the nominal value after every load change using a frequency restoration loop. The system frequencies without and with the frequency restoration loop are shown in Figures 11(a & b). As shown in Figure 11(a) the system frequency of the microgrid is reduced at 0.1 second and 1 second, and the frequency is maintained at the same level until the next injection of load or generation occurs. However, for the microgrid system with a frequency restoration loop, the system frequency is maintained at the nominal level, although there are some fluctuations for a small event during load injection or withdrawal.

Similarly, the neutral currents of the three-phase-four-wire microgrid are also observed, which identified that the loading of neutral affects the system in many ways. The currents in the neutral of DGs are found to be unequal while sharing an equal unbalanced load with the conventional virtual impedance loop based on $\alpha\beta$-axes. Whereas the DG neutral currents are observed to be equal with the proposed virtual impedance loop even while sharing the unbalanced load. The nature of neutral currents with both conventional and the proposed virtual impedance controller is shown in Figure 12(a & b). In Figure 12(a), an unequal distributed nature of neutral currents with different scaled values can be seen for the conventional controller, whereas the neutral currents of the DGs with proposed controller are found to be uniform with same scaled values (in Figure 12(b)).
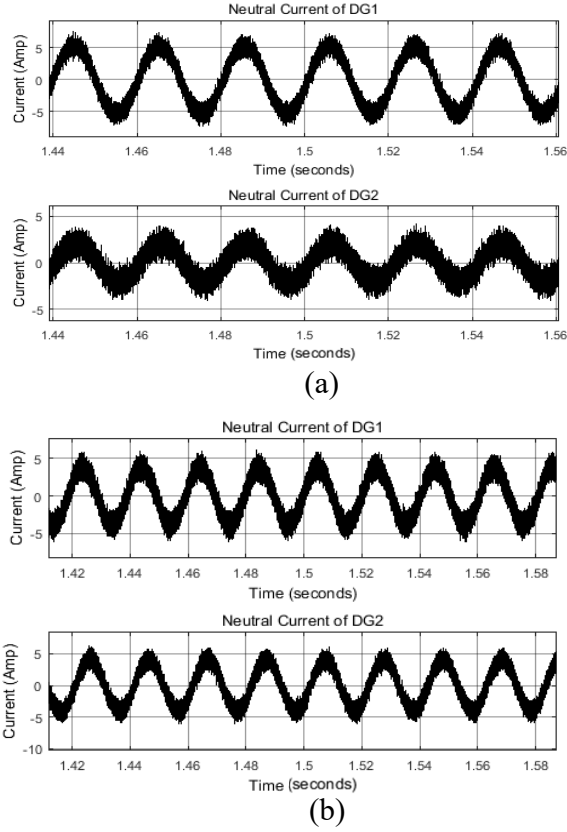
Figure 12: DG neutral currents: (a) With conventional VI loop, (b) With the proposed VI loop

## 3.2. Performance analysis for proportional power-sharing (ratio 1: 2)

This scenario demonstrates the efficacy of the proposed control technique in proportional power-sharing, where the loads are shared between the two DGs in the ratio of 1:2. To do this, a few changes are required in the controller parameters such as droop coefficients, virtual impedance, and inner controller gains. The droop coefficients of $DG_1$ and $DG_2$ are made in the ratio 2: 1, so that the power will be shared in the ratio of 1:2. The value of virtual impedance is the impedance difference of the lines for equal power-sharing; it is used in the DG, which has lower line impedance and shares more reactive power in the absence of virtual impedance. In this scenario, $DG_1$ has a lower line impedance so the virtual impedance should be applied to it. Moreover, it is required that $DG_1$ should share half of the load shared by $DG_2$, so the value of virtual impedance required for this scenario is double than that required in the previous scenario, as given in Equation (6). Hence, the load shared by $DG_2$ is double the load shared by $DG_1$. To have a similar transient load sharing response, the controller gains of $DG_1$ are selected half to those of $DG_2$. The simulation parameters used in this scenario are listed in Table 3. The simulation of the test system is run for three seconds with the unbalanced load connected to the system in the time interval from one second to two seconds. The results obtained for this scenario are described onwards.

Table 3: Simulation parameters used in scenario 2.

| Description of Parameters | Value | Remarks |
|---|---|---|
| Virtual Impedance $(R_v + jX_v)$ | $0.4 + j1.2$ | Used in $DG_1$ only |
| Droop Coefficients $m_p$, $m_i$, and $n$ for $DG_1$ | 0.0002, 0.002 and 0.0026 | For $DG_2$ same as used in scenario 1 |
| Voltage Controler Gains for DG₁, $K_p$, and $K_r$ | 0.225 and 17.5 | For $DG_2$ same as used in scenario 1 |
| Current Controler Gains for DG₁, $K_p$, and $K_r$ | 0.5 and 400 | For $DG_2$ same as used in scenario 1 |

Figure 13(a) shows the proportional active power-sharing with the proposed control technique. Despite the nature of the loads added or removed, the DG₂ has taken an active load which is clearly seen as double that shared by the DG₁. This proportional active power-sharing is consistent with the sharing ratio of 1:2 throughout the considered duration, and is not affected by the switching of unbalance load. On the other side, the proportional negative and positive sequence reactive power-sharing are shown in Figures 13(b & c). These Figures imply that the proposed VI loop also enabled an accurate negative and positive sequence proportional reactive power-sharing in the ratio of 1:2. Similar to the active power-sharing, each DG shares an equal reactive power despite the change in system reactive load. Moreover, the negative sequence reactive power is also shared in the expected 1:2 ratio, when the unbalanced loads are brought to the system in the time interval from one second to two seconds. The system's active and reactive loads are shared precisely in the ratio of 1:2 between the two DGs. Similarly, the DG currents are also observed in the same ratio. On the other side, the DG₂ current is seen as double of DG₁ current for this proportional power-sharing scenario, which can be seen in Figure 14. However, the DGs' terminal voltages remain unaffected in this case, and their waveforms are found to be similar to those in scenario 1.
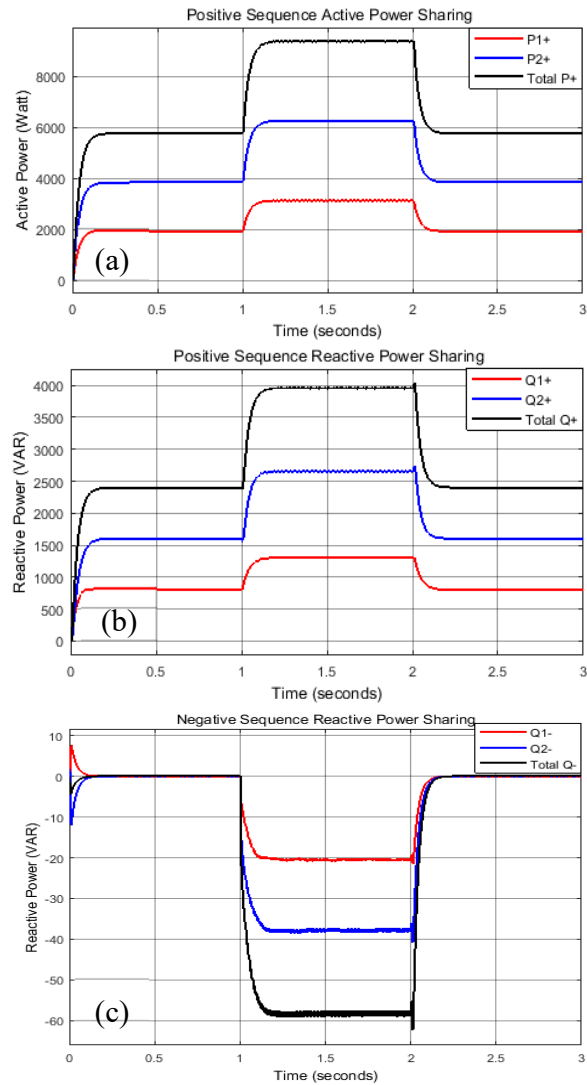
Figure 13: Proportional power-sharing (ratio 1:2): (a) Active power, (b) Positive sequence reactive power, (c) Negative sequence reactive power
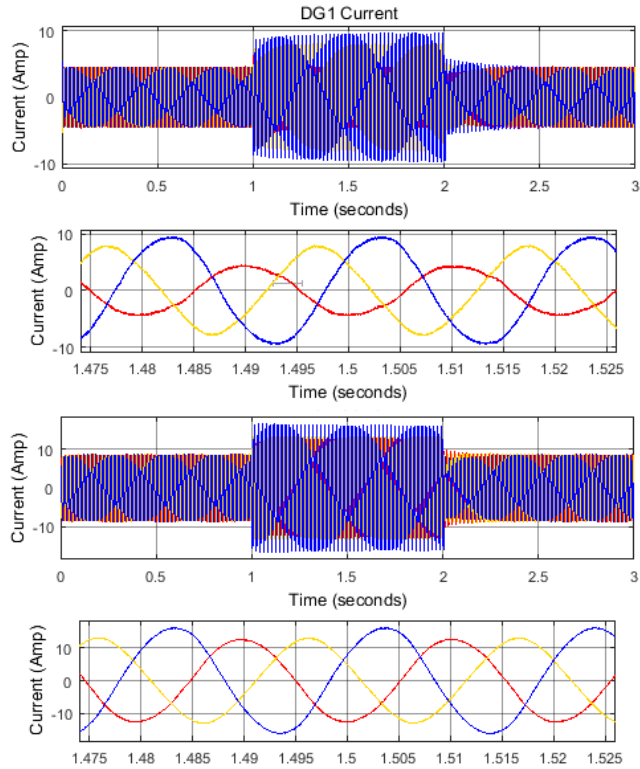
Figure 14: DG currents for proportional power-sharing (ratio 1:2)

## 3.3. Stability analysis of the proposed controller

In order to ensure the stability of the proposed controller while reaching good performance of the controller during both steady-states and transients, several root-loci sweeps have been performed on both the voltage and current control loops. The voltage and current control loops have been studies separately for simplicity of the analysis, since otherwise the global transfer function would be more complex and have a higher order. In such a case, Bode analysis may be not valid anymore. In order to separate the voltage and current loops, the external loop as shown in Figure 15, which is the one corresponding to the voltage need to have a significant lower bandwidth than the current one.
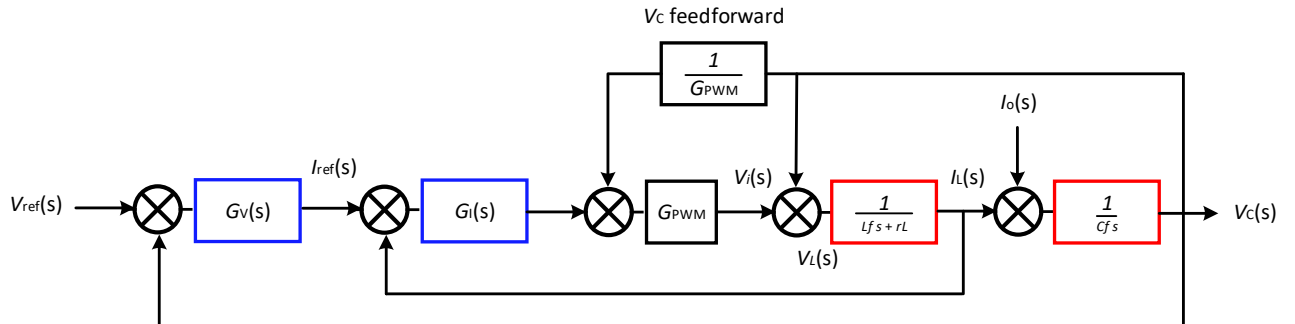


Figure 15: Simplified schematic of the whole system of one inverter in the s-domain.

As shown in Figure 16(a), as the proportional gain increases from 0.4 to 1.3, the undamped natural frequency $\omega_n$ decreases, while the same can be observed on the damped natural frequency $\omega_d$. At the same time, it can be observed from the zeros that they are being moved from the origin along the X-axis for the first three values (0.4, 0.7, and 1), which indicates that the system would have a lower overshoot, which is confirmed by Figure 16(b). Accordingly, the proportional gain of the current loop has been set to 1.



Figure 16: Root loci of the current loop considering KPi sweep, and the corresponding response in the time domain.

As it can be noticed from Figure 17(a), the zeros have imaginary components. It can be also observed from the same Figure that both the undamped natural frequency $\omega_n$ and the damped natural frequency $\omega_d$ increase with the increase of the resonant gain. So, the exaggeration of increasing such parameters may cause instability of the system. Nevertheless, for the swept values, the poles are still on the left side plane confirming the stability of the system. Accordingly, the resonant gain has been set to 800.
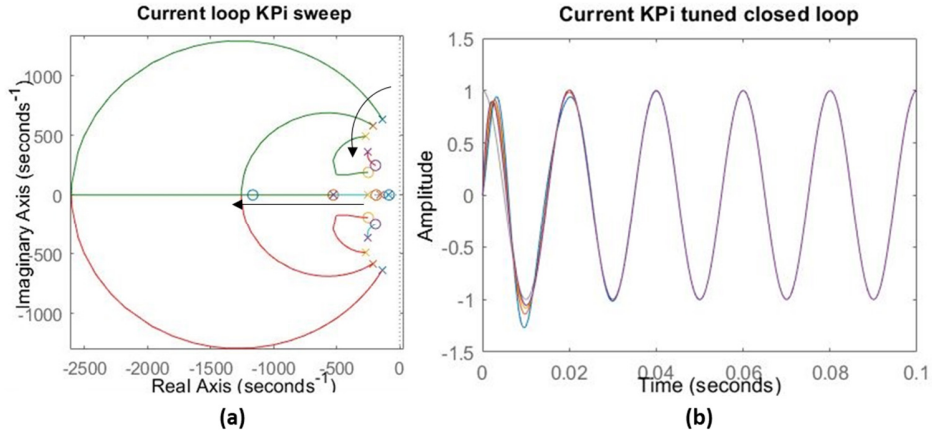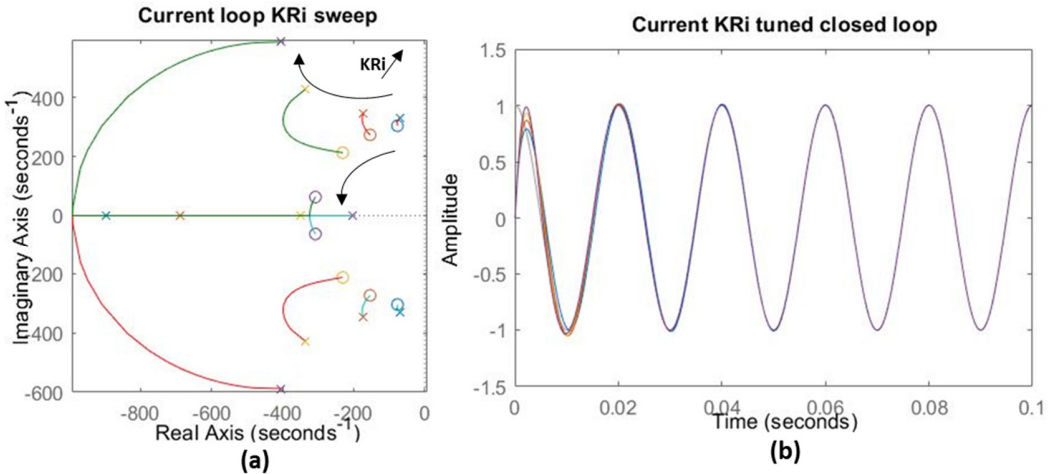


Figure 17: Root loci of the current loop considering KRi sweep, and the corresponding response in the time domain.

From the proportional gain sweep in the voltage loop, it can be seen that the poles are being moved further away from the origin along the X-axis indicating a better decay and damping, and a hence better stability. The same can be observed from the resonant gain damping. Although, the settling time of the system can be improved further, we have decided to stop at 0.45 and 35 for the proportional and resonant gain, respectively, in order to keep the bandwidth of the voltage loop lower enough than the one of the current loop, and thus preserving the inter loop stability. Accordingly, the voltage bandwidth was set to 79Hz, considering that the one of the current corresponds to 286Hz.
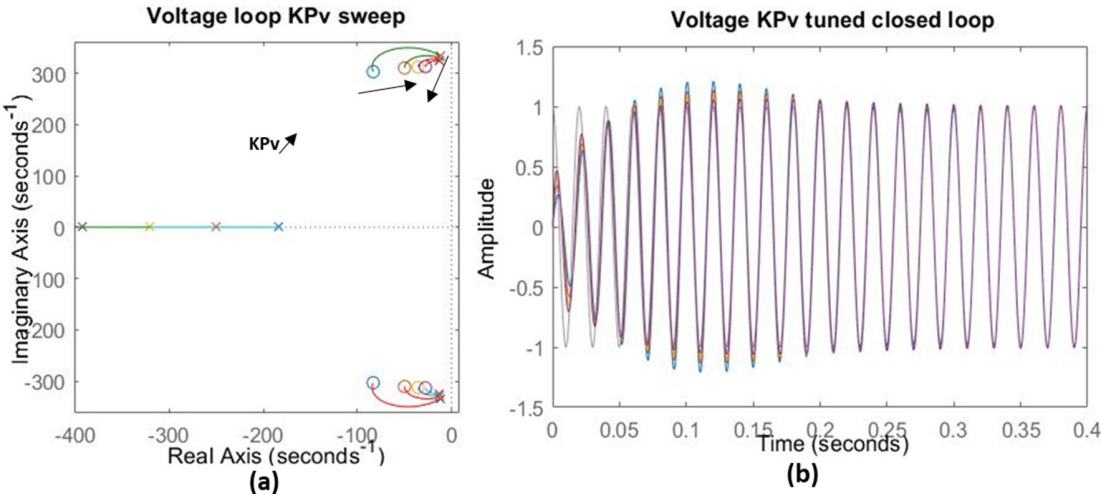


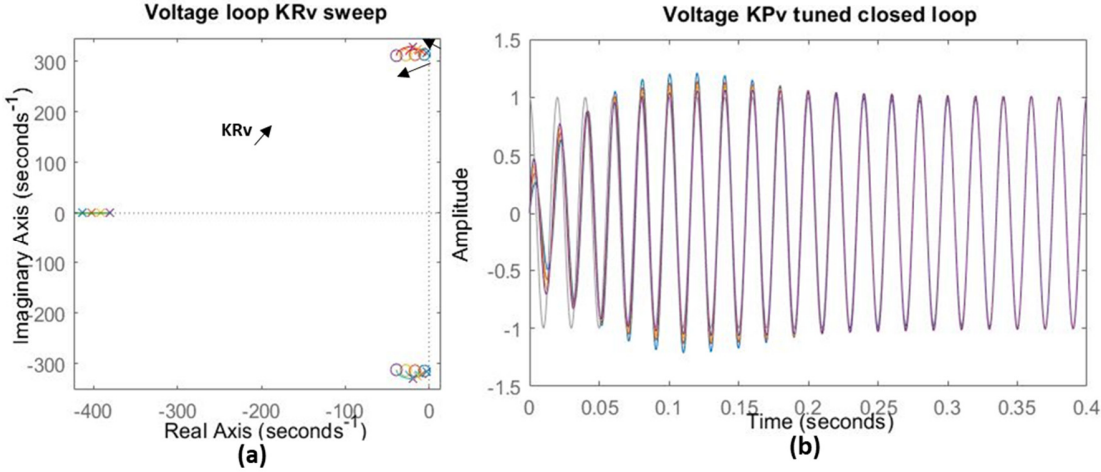Figure 18: Root loci of the current loop considering KPv sweep, and the corresponding response in the time domain.



Figure 19: Root loci of the current loop considering KRv sweep, and the corresponding response in the time domain.

## 3.4. Inferences

This sub-section is focused on the comparative outputs for different cases and methods, so that a complete application of the proposed method can be understood. For the first stage, as described in the 3.1 sub-section, the outputs of the conventional method are compared to the outputs from the proposed method. The outputs are presented and described in sub-section 3.1. However, in this sub-section, the improvements that we observed with the proposed method are listed and discussed thoroughly. Table 4 presents the comparisons of the methods based on different performance indexes. The main improvements that we found for the proposed control scheme over the conventional one are accurate negative current sharing, neutral current sharing, power quality, and sharing of unbalance loads. Similarly, the proposed control method is tried to apply in diverse scenarios and test cases, so that its robustness and practical implementation can be determined. For a complete comparison, the control method is tested for different proportional ratios, different numbers of DGs, and different simulation times, whose complete outcomes are listed in Table 5. With this comparison, it can be said that the proposed control scheme is one of the improved and practical methods, which can achieve the described objectives effectively.

Table 4: Comparison of performances for the proposed and conventional control scheme

| Description of parameter/performance | Conventional Method | Proposed Control Scheme |
|---|---|---|
| Active power-sharing | Accurate | Accurate |
| Positive sequence reactive power | Acceptable | Accurate |
| Negative sequence reactive power | Poor | Accurate |
| Neutral current sharing | Poor | Neutral currents are also shared in the load sharing ratio |
| Frequency deviation | Active load change dependent | Approximately constant |
| Sharing of unbalance | Poor | Acceptable |

Table 5: List of findings for different scenarios and their comparison

| Description of Scenario | Observations and Findings |
|---|---|
| Proportional sharing of sequence powers are carried out for the following ratios.<br><br>a) Ratio 1:2<br>b) Ratio 1:3<br>c) Ratio 1:4 | To demonstrate the ability of the proposed control scheme to share the unbalance, proportional sharing scenario has been considered. The significance of proportional sharing is that the capacities of interconnected DGs are different and share loads according to their capacities in the specified ratio. The proportional power-sharing is achieved by varying the droop coefficients, virtual impedance, and controller parameters according to the sharing ratio. The system load (balanced and unbalanced load) is constant for observation and is shared by two DGs in different proportions. Three observations for proportional power-sharing in the ratio 1:2, 1:3, and 1:4 are carried out. From the results, it is observed that the active power, being independent of voltage drop, is shared in the desired ratio with just |

| | the change in droop coefficients. However, reactive power sharing also required voltage drop modification according to the sharing ratio, which is achieved by the virtual impedance concept. As the virtual impedance is implemented considering both positive and negative components, it helps to achieve an accurate sharing of sequence reactive power. |
|---|---|
| The number of DGs in parallel is changed to<br><br>a) Two<br>b) Three<br>c) Four | Another basic requirement of a control strategy designed for a microgrid is the ability to cope with several units. The presented control strategy is implemented for a number of DGs operating in parallel. The performance of control strategy has been observed with two, three, and four DGs. The parallel DGs are assumed to have different line impedances. Virtual Impedances have been used in the controller of all DGs except the DG with the highest line impedance. The values of virtual impedances are different for each DG and depend on the difference between its line impedance and the highest impedance. From the results obtained, it is found that the proposed control strategy can share the unbalanced loads effectively even if four DGs are connected in parallel. Equal capacity DGs were considered for this case. Further, a balanced terminal voltage has been maintained in each DG while sharing the loads. |
| The observation time of the system has been increased to 15 seconds. | As suggested by the reviewers, the model has been run for a longer duration (15 seconds). From the results, it can be concluded that the effectiveness of the proposed control strategy doesn't degrade on a longer observation. The terminal voltages, active and reactive powers are seen as quite stable. Thus, the proposed control scheme is expected to be suitable for a long-duration operation. |

## 4. Conclusions

This paper shows you how to improve the performance of droop control under unbalanced loads if you have three-level NPC inverters that are used to make three-phase four-wire isolated microgrids. An impedance loop that is based on sequence components has been found to be very good at accurately sharing the positive and negative sequence components of power under balanced and unbalanced loads. In addition, the suggested method can balance the currents in the DGs' neutrals even if the sharing isn't even. Other than that, the frequency restoration loop makes sure that the system frequency stays within a very small range of the nominal frequency value (i.e., 50Hz). It has also been shown that the proposed method can share the sequence power with respect to the capacity of DGs, where the capacities are varied by changing the droop coefficients. Thus, it enables the proportional power-sharing in the ratios 1:1, 1:2, 1:3, 1:4, and so on. Similar results have been observed for multiple numbers of DGs (i.e., two DGs and four DGs), which show that the power-sharing effectiveness is not dependent on the number of DGs. One of the better and more practical ways to deal with unbalanced loading in isolated microgrid systems, the proposed control scheme, is found to be one of them.

## References

[1]     Y. Rajbhandari *et al.*, "Load prioritization technique to guarantee the continuous electric supply for essential loads in rural microgrids," *International Journal of Electrical Power & Energy Systems,* vol. 134, p. 107398, 2022.

[2]      Z. Hanzelka and Y. Varetsky, "Negative-sequence active power stream as an index of unbalance source," in *11th International Conference on Electrical Power Quality and Utilisation*, 2011: IEEE, pp. 1-4.

[3]      B. Shoeiby, R. Davoodnezhad, D. Holmes, and B. McGrath, "Voltage-frequency control of an islanded microgrid using the intrinsic droop characteristics of resonant current regulators," in *2014 IEEE Energy Conversion Congress and Exposition (ECCE)*, 2014: IEEE, pp. 68-75.

[4]     T. Vandoorn, J. De Kooning, B. Meersman, and L. Vandevelde, "Review of primary control strategies for islanded microgrids with power-electronic interfaces," *Renewable and Sustainable Energy Reviews,* vol. 19, pp. 613-628, 2013.

[5]      P. Piagi and R. H. Lasseter, "Autonomous control of microgrids," in *2006 IEEE Power Engineering Society General Meeting*, 2006: IEEE, p. 8 pp.

[6]     Q. Shafiee, J. M. Guerrero, and J. C. Vasquez, "Distributed secondary control for islanded microgrids—A novel approach," *IEEE Transactions on power electronics,* vol. 29, no. 2, pp. 1018-1031, 2013.

[7]     A. Shrestha and F. Gonzalez-Longatt, "Frequency stability issues and research opportunities in converter dominated power system," *Energies,* vol. 14, no. 14, p. 4184, 2021. [Online]. Available: https://www.mdpi.com/1996-1073/14/14/4184.

[8]      N. A. Ninad and L. A. Lopes, "Per-phase vector (dq) controlled three-phase grid-forming inverter for stand-alone systems," in *2011 IEEE International Symposium on Industrial Electronics*, 2011: IEEE, pp. 1626-1631.

[9]     J. He and Y. W. Li, "Analysis, design, and implementation of virtual impedance for power electronics interfaced distributed generation," *IEEE Transactions on industry Applications,* vol. 47, no. 6, pp. 2525-2538, 2011.

[10]    Y. A.-R. I. Mohamed and E. F. El-Saadany, "Adaptive decentralized droop controller to preserve power sharing stability of paralleled inverters in distributed generation microgrids," *IEEE Transactions on Power Electronics,* vol. 23, no. 6, pp. 2806-2816, 2008.

[11]    Q. Liu, Y. Tao, X. Liu, Y. Deng, and X. He, "Voltage unbalance and harmonics compensation for islanded microgrid inverters," *IET Power Electronics,* vol. 7, no. 5, pp. 1055-1063, 2014.

[12]    J. M. Guerrero, J. C. Vasquez, J. Matas, L. G. De Vicuña, and M. Castilla, "Hierarchical control of droop-controlled AC and DC microgrids—A general approach toward standardization," *IEEE Transactions on industrial electronics,* vol. 58, no. 1, pp. 158-172, 2010.

[13]     T. V. Hoang, T. D. Nguyen, and H.-H. Lee, "Adaptive virtual impedance control scheme to eliminate reactive power sharing errors in islanded microgrid," in *2016 IEEE International Conference on Sustainable Energy Technologies (ICSET)*, 2016: IEEE, pp. 224-229.

[14]  X. Zhao, X. Wu, L. Meng, J. M. Guerrero, and J. C. Vasquez, "A direct voltage unbalance compensation strategy for islanded microgrids," in *2015 IEEE Applied Power Electronics Conference and Exposition (APEC)*, 2015: IEEE, pp. 3252-3259.

[15]  W. Feng, K. Sun, Y. Guan, J. M. Guerrero, and X. Xiao, "Active power quality improvement strategy for grid-connected microgrid based on hierarchical control," *IEEE Transactions on Smart Grid,* vol. 9, no. 4, pp. 3486-3495, 2016.

[16]  B. Ren, X. Sun, S. Chen, and H. Liu, "A compensation control scheme of voltage unbalance using a combined three-phase inverter in an islanded microgrid," *Energies,* vol. 11, no. 9, p. 2486, 2018.

[17]  A. Vijay, S. Doolla, and M. C. Chandorkar, "Unbalance mitigation strategies in microgrids," *IET Power Electronics,* vol. 13, no. 9, pp. 1687-1710, 2020.

[18]  Y. Jia, D. Li, and Z. Chen, "Unbalanced power sharing for islanded droop-controlled microgrids," *Journal of Power Electronics,* vol. 19, no. 1, pp. 234-243, 2019.

[19]  N.-Y. Dai, M.-C. Wong, and Y.-D. Han, "Application of a three-level NPC inverter as a three-phase four-wire power quality compensator by generalized 3DSVM," *IEEE Transactions on power electronics,* vol. 21, no. 2, pp. 440-449, 2006.

[20]  P. Rodriguez, A. V. Timbus, R. Teodorescu, M. Liserre, and F. Blaabjerg, "Flexible active power control of distributed power generation systems during grid faults," *IEEE transactions on industrial electronics,* vol. 54, no. 5, pp. 2583-2592, 2007.

[21]  A. S. Pabbewar and M. Kowsalya, "Three level neutral point clamped inverter using space vector modulation with proportional resonant controller," *Energy Procedia,* vol. 103, pp. 286-291, 2016.

[22]  M. Hojabri, M. Hojabri, and A. Toudeshki, "Passive damping filter design and application for three-phase PV grid-connected inverter," *International Journal of Electrical, Electronics and Data Communication,* vol. 3, no. 6, pp. 50-56, 2015.

[23]  R. N. Beres, X. Wang, M. Liserre, F. Blaabjerg, and C. L. Bak, "A review of passive power filters for three-phase grid-connected voltage-source converters," *IEEE Journal of Emerging and Selected Topics in Power Electronics,* vol. 4, no. 1, pp. 54-69, 2015.

[24]  P. Rodriguez, R. Teodorescu, I. Candela, A. V. Timbus, M. Liserre, and F. Blaabjerg, "New positive-sequence voltage detector for grid synchronization of power converters under faulty grid conditions," in *2006 37th IEEE Power Electronics Specialists Conference*, 2006: IEEE, pp. 1-7.

[25]  J. M. Guerrero, J. Matas, L. G. D. V. De Vicuna, M. Castilla, and J. Miret, "Wireless-control strategy for parallel operation of distributed-generation inverters," *IEEE Transactions on Industrial Electronics,* vol. 53, no. 5, pp. 1461-1470, 2006.

[26]  M. Savaghebi, A. Jalilian, J. C. Vasquez, and J. M. Guerrero, "Autonomous voltage unbalance compensation in an islanded droop-controlled microgrid," *IEEE Transactions on Industrial Electronics,* vol. 60, no. 4, pp. 1390-1402, 2012.

[27]  L. F. A. Pereira and A. S. Bazanella, "Tuning rules for proportional resonant controllers," *IEEE Transactions on Control Systems Technology,* vol. 23, no. 5, pp. 2010-2017, 2015.

[28]  X. Zhou, F. Tang, P. C. Loh, X. Jin, and W. Cao, "Four-leg converters with improved common current sharing and selective voltage-quality enhancement for islanded microgrids," *IEEE Transactions on Power Delivery,* vol. 31, no. 2, pp. 522-531, 2015.